ACCOUNTS
of chemical research

Computational Vibrational Spectroscopy of Peptides and Proteins in One and Two Dimensions

JONGGU JEON, SEONGEUN YANG, JUN-HO CHOI, AND MINHAENG CHO*

Department of Chemistry and Center for Multidimensional Spectroscopy, Korea University, Seoul 136-701, Korea

RECEIVED ON JANUARY 12, 2009

Downloaded by RENMIN UNIV OF CHINA on October 2, 2009 | http://pubs.acs.org
Publication Date (Web): May 20, 2009 | doi: 10.1021/ar900014e

CONSPECTUS

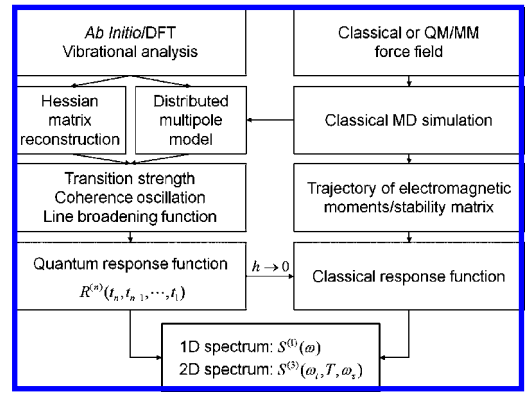

Vibrational spectroscopy provides direct information on molecular environment and motions but, its interpretation is often hampered by band broadening. Over the past decade, two-dimensional (2D) vibrational spectroscopy has emerged as a promising technique to overcome a number of difficulties associated with linear spectroscopy and provided significantly detailed information on the structure and dynamics of complex molecules in condensed phases. This Account reviews recently developed computational methods used to simulate 1D and 2D vibrational spectra. The central quantity to calculate in computational spectroscopy is the spectroscopic response function, which is the product of many contributing factors such as vibrational transition energies, transition moments, and their modulations by fluctuating local environment around a solute. Accurate calculations of such linear and nonlinear responses thus require a concerted effort employing a wide range of methods including electronic structure calculation (ESC) and molecular dynamics (MD) simulation. The electronic structure calculation can provide fundamental quantities such as normal-mode frequencies and transition multipole strengths. However, since the treatable system size is limited with this method, classical MD simulation has also been used to account for the dynamics of the solvent environment. To achieve chemical accuracy, these two results are combined to generate time series of fluctuating transition frequencies and transition moments with the distributed multipole analysis, and this particular approach has been known as the hybrid ESC/MD method. For coupled multichromophore systems, vibrational properties of each chromophore such as a peptide are individually calculated by electronic structure methods and the Hessian matrix reconstruction scheme was used to obtain local mode frequencies and couplings of constituting anharmonic oscillators. The spectra thus obtained, especially for biomolecules including polypeptides and proteins, have proven to be reliable and in good agreement with experimental spectra. An alternative to the hybrid method has also been developed, where the classical limit of the vibrational response function was considered. Its main attraction is the capability to obtain the spectra directly from a set of MD trajectories. A novel development along this direction has been achieved by using quantum mechanical/molecular mechanical (QM/MM) force fields for the accurate description of vibrational anharmonicity and chromophore polarization effects. The latter aspects are critical in the 2D case because classical force fields employing harmonic intramolecular potential cannot produce reliable 2D signal. We anticipate that the computational methods presented here will continue to evolve along with experimental advancements and will be of use to further elucidate ultrafast dynamics of chemical and biological systems.

Introduction

Vibrational spectroscopy is a powerful technique for the studies of microscopic structure and dynamics of molecules. Two-dimensional (2D) vibrational spectroscopy employing multiple IR pulses probes multiple quantum transitions and the observed signal in the 2D frequency space can

Published on the Web 05/20/2009 www.pubs.acs.org/acr
10.1021/ar900014e CCC: $71.50 © 2009 American Chemical Society

provide detailed information on vibrational mode anharmonicity, coupling between modes, and homogeneous and inhomogeneous line broadenings. Thus, 2D IR spectroscopy, which is an optical analogue of heteronuclear 2D NMR,[1] has been increasingly used to study solvation and hydrogen bonding dynamics, chemical exchange reactions, and peptide and protein structure and dynamics.[2−10]

A critical step in the interpretation of vibrational spectra is the understanding of the microscopic origin of various spectral features. In this regard, theoretical modeling and computation have played an essential role. From a theoretical perspective, the spectroscopic observable B is determined by the response function $R^{(n)}$ as[11]

$$B(t) = \int_0^\infty dt_n \ldots \int_0^\infty dt_1\, R^{(n)}(t_n, \ldots, t_1)\, F_n(t - t_n) \ldots F_1(t - t_n \ldots - t_1) \quad (1)$$

where the external electromagnetic fields are denoted as $F_n(t)$. The linear spectroscopy corresponds to $n = 1$, and a general four-wave mixing scheme is associated with the case $n = 3$. Time-dependent perturbation theory yields the response function as nested quantum commutators of electronic multipole or polarizability operators at different times and its evaluation requires a proper account of quantum states as well as the system dynamics.

The hybrid electronic structure calculation/MD (ESC/MD) simulation method combined with fragment approximation provides a reliable way to simulate and interpret 1D and 2D spectra of small chromophores in solution.[8,12,13] An alternative to the preceding approach is to take the classical limit of the response functions for IR absorption and vibrational circular dichroism (VCD) and evaluate it directly from MD simulation.[14−16] An analogous approach applied to nonlinear vibrational spectroscopy has also been developed in terms of the classical limit of the relevant nonlinear response function.[17] So far, this *direct MD* method has been mainly used to simulate fifth-order Raman spectra of liquid intermolecular modes[18,19] and 2D IR surface spectra of adsorbates.[20] Its novel application to the 2D IR spectroscopy in solution will be described in the present Account.

The two approaches mentioned above, the hybrid ESC/MD and the direct MD methods, can be contrasted in many respects. First, the hybrid method retains the quantum nature of vibrational transitions and nuclear dynamics unlike the direct method that is fundamentally classical. Thus, the nonlinear spectra from the latter need careful interpretation in terms of quantum-classical correspondence. Nevertheless, the direct method is advantageous in that the entire spectrum covering many vibrational modes can be obtained at once including the 2D cross peaks between modes. With the hybrid ESC/MD method, the properties of all modes of interest and their couplings need to be modeled individually. In addition, an important issue of computational spectroscopy has been the accurate description of vibrational anharmonicity, especially in the 2D IR spectroscopy that strongly reflects the anharmonic part of the potential energy.[4,21] In the hybrid method, this is achieved by ESC and theoretical modeling of intermode interactions and solvatochromism. In the direct method, the quantum mechanical/molecular mechanical (QM/MM) force field[22] is shown to be essential in capturing the anharmonicity. In this Account, the two methods will be discussed with a few applications to 1D and 2D IR spectroscopy of peptides and proteins.

Hybrid Electronic Structure Calculation/MD Simulation

The protein amide I mode has been extensively studied to probe protein structure and dynamics because its vibrational spectra sensitively reflect the backbone structure of polypeptides.[10,23−25] Below, a computational procedure called the *hybrid ESC/MD* method[8] is described, which is based on the Frenkel exciton or coupled-anharmonic-oscillator model of interacting anharmonic oscillators and provides the vibrational response function of polypeptides in solution.

Hessian Matrix Reconstruction and Fragment Approximation. The necessary parameters of the model such as the local vibrational frequencies and the intermode coupling constants have been determined by carrying out Hessian matrix reconstruction (HMR) analyses of ESC results on small oligopeptides.[8] The *ab initio* geometry optimization and vibrational analysis of a polypeptide produce the amide I normal-mode frequencies and eigenvectors in the atomic basis of size $3N_a$, where N_a is the number of atoms in the polypeptide. The corresponding Hessian matrix $F^{(0)}$ in the mass-weighted Cartesian coordinates can be diagonalized by a unitary matrix U as $U^{-1}F^{(0)}U = \Lambda$. Now, it is assumed that the eigenvector of the jth amide I local mode is fully determined by the eigenvector elements associated with the six atoms, O(═C), C(═O), N(−H), H(−N), C_α, and H($-C_\alpha$), that constitute the jth peptide bond. By denoting the corresponding eigenvector elements as U_{mj}, where m represents Cartesian components of the six atoms above, the Hessian matrix in the amide I local mode subspace can be obtained as

$$\bar{F}_{ij} = \sum_{n,m} U^{-1}_{i,n} F^{(0)}_{nm} U_{mj} \quad (2)$$

Downloaded by RENMIN UNIV OF CHINA on October 2, 2009 | http://pubs.acs.org
Publication Date (Web): May 20, 2009 | doi: 10.1021/ar900014e

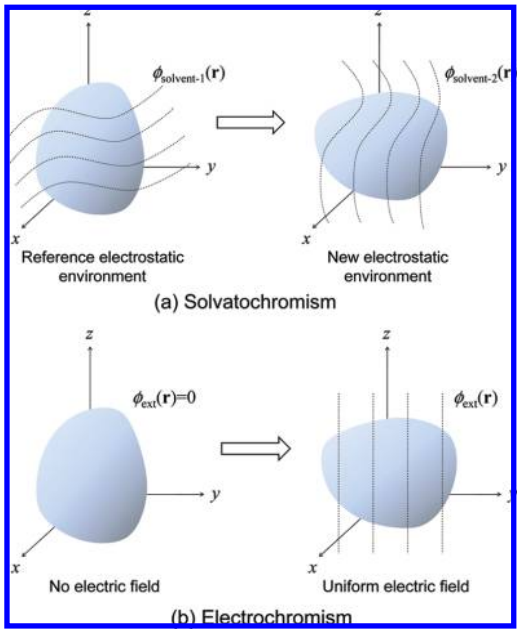

FIGURE 1. (a) Solvatochromism: The vibrational properties of a solute molecule change in response to the electrostatic potential generated by the local environment. (b) Electrochromism (vibrational Stark effect): As a special case of solvatochromism, the solute vibrational properties change by the external uniform electric field.

The diagonal and off-diagonal matrix elements of $\bar{F}$ correspond to the amide I local mode and coupling force constants, respectively. This HMR procedure has been successfully applied to dipeptides, short polypeptides, secondary structure polypeptides, and protein ubiquitin.[13,26] Then, within the fragment approximation, the transition electric and magnetic dipole moments of amide I vibrations are approximated as linear combinations of those of properly chosen unit peptides.[8,27]

Solvatochromism: Amide I Frequency Shift and Fluctuation. Solute−solvent interaction is responsible for numerous spectroscopic phenomena. Particularly, vibrational frequency shift induced by highly inhomogeneous local electric field produced by solvent molecules is known as vibrational solvatochromism[28] (Figure 1(a)), whereas that induced by external static electric field is as vibrational electrochromism or Stark effect[29] (Figure 1(b)).

To understand the solute−solvent interaction-induced effects on vibrational spectra, one needs theoretical models for vibrational frequency shift and its fluctuation in time.[8] The time-correlation function of the latter is an essential ingredient for numerical simulations of 1D and 2D vibrational spectra. A general framework to describe solvatochromism has been presented recently, where the charge distribution of the solute interacting with solvent electric field is divided into multiple fragments.[30] According to this, the frequency shift of *j*th mode is given by the following expansion in terms of distributed multipole moments of solute charge distribution,[30]

$$\Delta\omega_j(\phi) = \sum_x l_{xj}\phi(\mathbf{R}_x) + \sum_x \mathbf{L}_{xj}\cdot\mathbf{E}(\mathbf{R}_x) + \sum_x \Lambda_{xj}:\nabla\mathbf{E}(\mathbf{R}_x) + \ \ldots \ (3)$$

where $\mathbf{R}_x$ is the position of fragment x and ϕ and $\mathbf{E}$ represent the local electric potential and field, respectively, at the fragment site due to the environment. Note that these distributed sites collectively act like an antenna sensing local electric field around a solute. The three coefficients in eq 3 are

$$l_{xj} = (\hat{F}_j q_x(\mathbf{Q}))_{\mathbf{Q}_0},$$
$$\mathbf{L}_{xj} = -(\hat{F}_j \mathbf{p}_x(\mathbf{Q}))_{\mathbf{Q}_0},$$
$$\text{and}\ \ \Lambda_{xj} = -\frac{1}{6}(\hat{F}_j \Theta_x(\mathbf{Q}))_{\mathbf{Q}_0} \qquad (4)$$

with

$$\hat{F}_j \equiv \frac{1}{2M_j\omega_j}\left\{\frac{\partial^2}{\partial Q_j^2} - \sum_i \frac{g_{ijj}}{M_i\omega_i^2}\frac{\partial}{\partial Q_i}\right\} \qquad (5)$$

Here, M_j, ω_j and Q_j are, respectively, the reduced mass, frequency and the coordinate of the *j*th normal mode, g_{ijj} is the cubic anharmonic coefficient, q_x, $\mathbf{p}_x$, and $\mathbf{\Theta}_x$ are, respectively, the partial charge, dipole moment, and quadrupole moment of fragment x, and the partial derivatives are evaluated at the equilibrium position $\mathbf{Q}_0$ of an isolated molecule. The first term in eq 5 describes the nonlinear coordinate dependencies of distributed multipoles, whereas the second does the mechanical anharmonicity contributions to the solvatochromism.

For the amide I mode of polypeptide, its frequency is redshifted in solution due to hydrogen bonding interaction with water and also the band broadens because of the solvent-induced frequency fluctuations. This solvatochromic effect has been quantitatively described by the model in eq 3 truncated after the monopole term (distributed charge approximation) with the four atomic sites, O(═C), C(═O), N(−H), and H(−N), as the expansion centers.[31] The amide I frequency shift due to surrounding water molecules then becomes

$$\delta\omega_j^I(t) = \sum_{x=1}^{4} l_x \phi_{x(j)}^{\text{water}}(t) \qquad (6)$$

where $\phi_{x(j)}^{\text{water}}(t)$ is the Coulomb potential at site x of the *j*th peptide bond at time t. The coefficients l_x were determined by linear regression analysis of the *ab initio* results on a number of peptide−water clusters. Once the snapshot configurations of the polypeptide−water system are obtained from MD trajec-

Downloaded by RENMIN UNIV OF CHINA on October 2, 2009 | http://pubs.acs.org
Publication Date (Web): May 20, 2009 | doi: 10.1021/ar900014e

tories, the solvatochromic amide I local mode frequency trajectories can be obtained with eq 6. This method has been successfully applied to various *N*-methylacetamide (NMA)−water clusters, NMA dissolved in water and methanol, and polypeptides and ubiquitin in water.[8,32−34]

Solvatochromism and Vibrational Stark Effect. In the vibrational Stark effect spectroscopy, the change in IR absorption upon application of external electric field is measured.[35−37] The key quantities are the vibrational Stark tuning rate $\Delta\boldsymbol{\mu}$ and the transition polarizability **A**, which are the first order contributions to the changes in the frequency and transition dipole moment, respectively.[29] This has been utilized recently to probe local electric field at an enzyme active site.[38] Recently, an expression for the vibrational Stark tuning rate was provided by using the general solvatochromic frequency shift in eq 3 with the substitution of the uniform electric field and corresponding electrostatic potential, i.e., for the *j*th mode,[30]

$$\Delta\mu_j = \hbar\sum_x (l_{xj}\mathbf{R}_x + \mathbf{L}_{xj}) \tag{7}$$

and, using eq 4, it becomes

$$\Delta\mu_j = (\hat{F}_j\mathbf{D}_g(\mathbf{Q}))_{\mathbf{Q}_0} = \frac{\hbar}{2M_j\omega_j}\left(\frac{\partial^2\mathbf{D}_g(\mathbf{Q})}{\partial Q_j^2}\right)_{\mathbf{Q}_0} - \frac{\hbar}{2M_j\omega_j}\sum_i \frac{g_{iij}}{M_i\omega_i^2}\left(\frac{\partial\mathbf{D}_g(\mathbf{Q})}{\partial Q_i}\right)_{\mathbf{Q}_0} \tag{8}$$

where $\mathbf{D}_g(\mathbf{Q})$ is the ground state dipole moment of an unperturbed molecule. Thus, the vibrational Stark tuning rate can be calculated by the parameters used to describe the solvatochromic frequency shift. For the amide I vibration of NMA, the parameters from the distributed charge analysis[12] yield $|\Delta\boldsymbol{\mu}_j| = 0.78$ cm^{-1}/(MV/cm), which is close to available experimental data on typical stretching modes of CN, SCN, and azido groups. The observation that the direction of $\Delta\boldsymbol{\mu}_j$ is very close to that of amide I transition dipole $(\partial\mathbf{D}_g(\mathbf{Q})/\partial Q_j)_{\mathbf{Q}_0}$ indicates that the second term in eq 8, which originates from potential anharmonicity of amide I mode itself, g_{jjj} for j = amide I mode, may be dominant. For the other vibrational modes for which the distributed charge model parameters are available,[39,40] the calculated $|\Delta\boldsymbol{\mu}_j|$ are as follows (in cm^{-1}/(MV/cm)): 0.31 (CN stretch of CH_3CN), 0.54 (CN stretch of CH_3SCN), 0.48 (N_3 stretch of CH_3N_3). These values agree very well with experimental data[36,37] on $|\Delta\boldsymbol{\mu}_j|f$ (0.43, 0.71, and 0.54[41] for the three modes, respectively), once the typical value of 1.1−1.3 for the local field correction factor f is allowed for. Although these comparisons demonstrate that the electrochromism can be described by the solvatochromic model parameters, the reverse is not always true because solvatochromism involving spatially nonuniform solvent electric field is inherently more complicated than the uniform electric field effect in electrochromism.

IR, VCD and 2D IR Spectroscopy of Polypeptide Amide I Vibrations. The IR and VCD spectra of a polypeptide with *N* amide I normal modes can be obtained by Fourier transforming the weighted linear response functions as

$$I_{\mathrm{IR/VCD}}(\omega) = \int_{-\infty}^{\infty} \mathrm{d}t\, \mathrm{e}^{\mathrm{i}\omega t}\sum_{\alpha=1}^{N} D_\alpha\, \mathrm{e}^{-\mathrm{i}\bar{\omega}_\alpha t}J_\alpha(t) \tag{9}$$

where $\bar{\omega}_\alpha$ is the ensemble-averaged αth amide I normal mode transition frequency and the linear response function $J_\alpha(t)$ describes the vibrational coherence decay of the same mode. For IR spectra, $D_\alpha \equiv |(\partial\boldsymbol{\mu}/\partial Q_\alpha)|^2$ is the dipole strength and, for VCD, it represents the rotational strength, Im $[(\partial\boldsymbol{\mu}/\partial Q_\alpha)\cdot(\partial\mathbf{m}/\partial Q_\alpha)]$, where $\boldsymbol{\mu}$ and **m** are electric and magnetic dipole moments, respectively. Equation 9 involves approximate perturbative treatments of the solvent-induced transition frequency fluctuations and normal modes,[42] but the generalization including nonadiabatic effects has also been reported.[43,44] Combining the classical MD simulation with the distributed charge model given in eq 6, one can obtain the frequency trajectories for all amide I local modes in a given polypeptide. Within the adiabatic approximation, the linear response function can be calculated by using the frequency−frequency correlation functions and the IR and VCD spectra of small oligopeptides and proteins were numerically simulated.[13,45]

In Figure 2, the IR and VCD spectra of six different secondary structure model polypeptides with 21 alanine residues are plotted. The amide I IR spectra of right-handed α-helix (RHH), antiparallel β-strand (APB), parallel β-strand (PB), and polyproline II (P_{II}) appear to be broad and featureless, whereas those of π-helix (πH) and 3−10 helix (3_{10}H) exhibit a doublet pattern. Although the latter spectra show notable peak patterns, the amide I IR absorption spectroscopy does not provide enough information to precisely and uniquely determine the polypeptide secondary structure. In contrast, the VCD spectra in Figure 2(b) are distinctively different from one another. Particularly, our results are consistent with the experimentally measured VCD spectra of RHH and P_{II} polypeptides exhibiting (−,+,−) and (−,+) peak patterns, respectively.[46] The three extended structure polypeptides, P_{II}, APB, and PB, show the same (−,+) pattern, when the spectrum is read from low to high frequency region. Therefore, the VCD technique can bet-

Downloaded by RENMIN UNIV OF CHINA on October 2, 2009 | http://pubs.acs.org
Publication Date (Web): May 20, 2009 | doi: 10.1021/ar900014e

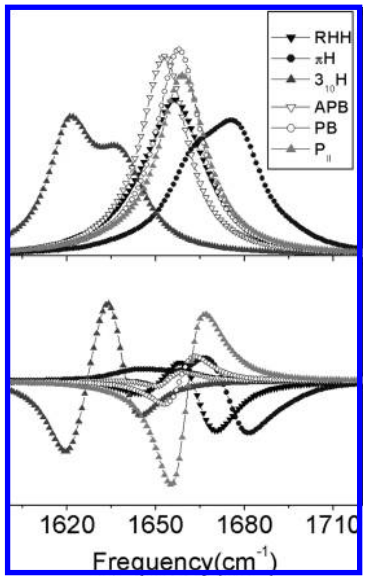

FIGURE 2. Simulated amide I IR (a) and VCD (b) spectra of six different secondary structure polypeptides with 21 alanine residues in water. Reprinted with permission from ref 42. Copyright 2006 John Wiley & Sons, Inc.

ter distinguish the helical conformations from the extended structure than the IR absorption.

The 2D IR spectrum exhibits not only diagonal peaks revealing amide I mode transition frequencies but also cross peaks determined by intermode couplings that are sensitive to detailed 3D protein structure.[10,47,48] Particularly, by using beam polarization-controlled 2D IR techniques,[48] the 2D IR difference spectrum has been measured where the diagonal peaks are selectively eliminated. It was found that the cross peak amplitude in a given 2D IR difference spectrum is mainly determined by the factor Φ_{jk}, defined as the product of the two dipole strengths and angle-dependent sin^2 term,[8]

$$\Phi_{jk} \equiv |\mu_{e_j g}|^2 |\mu_{e_k g}|^2 \sin^2 \theta_{e_k, e_j} \qquad (10)$$

where e_j and f_k denote the jth singly excited state and the kth doubly excited, either combination or overtone, state, respectively and θ_{e_k,e_j} is the angle between the transition dipoles of the jth and kth states. In ref 49, the above rule was used to distinguish the parallel and antiparallel forms of β-sheet polypeptides. Equation 10 can be an important guideline for quantitatively describing the relative amplitudes of different cross peaks in the secondary structure polypeptides and ubiquitin spectra.[8,13,49]

Although the parallel-polarization 2D IR spectra, where all the incident beam polarization directions are parallel, are not shown here, their spectra are overall similar to one another, while one can clearly see the differences in the 2D difference spectra of those polypeptides in Figure 3.

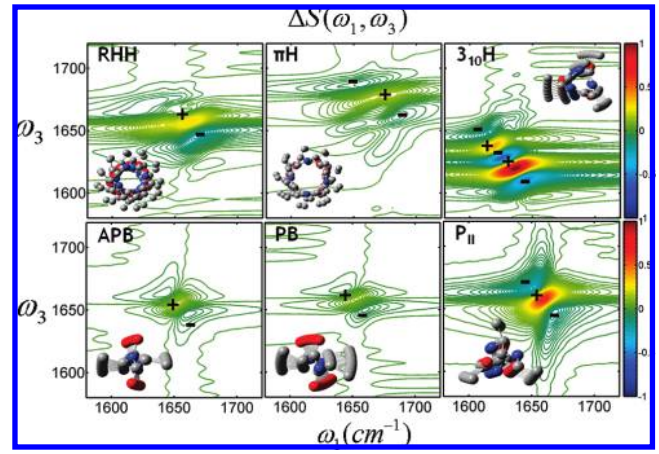

FIGURE 3. 2D IR difference spectra of six different secondary structure polypeptides. $\Delta S = S_{\parallel} - 3S_{\perp}$ ($S_{\parallel}$ and $S_{\perp}$ are rephasing signals with parallel and perpendicular polarizations, respectively) corresponds to four waves having polarization directions $[0,\pi/3,-\pi/3,0]$.[48] Reprinted with permission from ref 42. Copyright 2006 John Wiley & Sons, Inc.

First, the amplitudes of the $\Delta S(\omega_\tau,\omega_t)$ spectra of RHH and πH are much smaller than that of 3_{10}H. Second, the two cross peaks are visible in the 3_{10}H spectrum. In the 2D IR difference spectra of the three extended structures, the cross peak amplitudes in the P$_{II}$ $\Delta S(\omega_\tau,\omega_t)$ spectrum are much stronger than those of the APB and PB. The origin of the different structure−spectrum relationships observed in Figure 3 can be understood from detailed analyses of delocalized amide I normal modes and eq 10 which keenly reflects the polypeptide structure.

Although the 2D IR and electronic spectroscopy based on a stimulated photon echo measurement technique has certain advantages in terms of frequency and time resolutions over linear spectroscopic methods, the measured signals are not sensitive to molecular chirality in solution. Recently, novel 2D optical spectroscopic methods using circularly polarized (CP) beams were theoretically proposed and shown to be useful in measuring nonlinear optical activity of chiral molecules in an isotropic medium.[8,45,50] As VCD spectroscopic measurements provide additional information such as peak signs, 2D CP-IR photon echo spectroscopy can be a better tool for protein structure determination than 2D IR PE spectroscopy.[45]

Direct Calculation of Spectroscopic Correlation Functions with QM/MM MD

QM/MM MD Simulation and Dipole Correlation Functions. Spectroscopic properties of a molecule in solution are the consequences of incessant structural and electronic fluctuations of the solute molecule, which occur in tandem with the solvent motions. The quantum mechanical treatment of the *solute* dynamics would thus be the first step

Downloaded by RENMIN UNIV OF CHINA on October 2, 2009 | http://pubs.acs.org
Publication Date (Web): May 20, 2009 | doi: 10.1021/ar900014e

to extract the microscopic information from the observed spectra, ahead of the full quantum mechanical inspection of the entire solute−solvent system. The combined QM/MM method[51] has thus been widely used to study reaction mechanisms, thermodynamics properties, and structure of molecular systems. The QM/MM MD method intertwines the advantages of the QM and the MD techniques and generates a dynamics trajectory evolving under an effective Hamiltonian

$$\hat{H}_{\text{eff}} = \hat{H}_{\text{QM}} + \hat{H}_{\text{MM}} + \hat{H}_{\text{QM/MM}} + \hat{H}_{\text{boundary}} \qquad (11)$$

with the interaction Hamiltonian $\hat{H}_{\text{QM/MM}}$ given as the sum of Coulomb and dispersion−repulsion interactions between the QM and MM subsystems.

We utilize the QM/MM MD method to simulate the vibrational spectra of small peptides in solution with QM peptide and MM solvent. The atomic partial charges are obtained from the charge distributions at every time step via the Mulliken or Löwdin population analyses. The electric dipole moment is defined by $\boldsymbol{\mu}(t) = \sum_j q_j(t)\, \mathbf{r}_j(t)$, where q_j and $\mathbf{r}_j$ are the partial charge and the position of the jth QM atom. Note that both q_j and $\mathbf{r}_j$ fluctuate in time. The dipole−dipole autocorrelation function is then Fourier-transformed to give the IR absorption spectrum

$$I(\omega) = \frac{N_0}{2\pi}\int_{-\infty}^{\infty} dt\, e^{-i\omega t}\langle \boldsymbol{\mu}(0)\cdot\boldsymbol{\mu}(t)\rangle \qquad (12)$$

where N_0 is the number density and $\langle ...\rangle$ denotes ensemble average. Next, the VCD spectrum calculation requires the magnetic dipole $\mathbf{m}(t) = (1/2c)\sum_j q_j(t)\, \mathbf{r}_j(t) \times \mathbf{v}_j(t)$, where c is the speed of light and $\mathbf{v}_j$ is the velocity of the jth QM atom. The VCD line shape function is the imaginary part of the Fourier-transformed cross-correlation function of the electric and magnetic dipole moments, i.e.,[14,52]

$$\Delta I(\omega) = \frac{N_0}{\pi}\text{Im}\int_{-\infty}^{\infty} dt\, e^{-i\omega t}\langle \boldsymbol{\mu}(0)\cdot\mathbf{m}(t)\rangle \qquad (13)$$

which is again evaluated from QM/MM MD trajectories.

Direct Simulations of IR and VCD Spectra of Small Model Peptides. Figure 4(a) shows the simulated IR absorption spectra of NMA in H_2O (black line) and *N*-deuterated NMA in D_2O (gray line) solution obtained using the QM/MM MD method[15] with the semiempirical AM1 approximation for the solute and the TIP3P water model.

The amide modes spanning up to ~4000 cm^{-1} are resolved with 1 fs time step. We focus on the amide modes below 2000 cm^{-1} in this Account. For comparison, the IR spectra obtained with classical force field having fixed solute partial charges are given in Figure 4(a)-a. The classical results

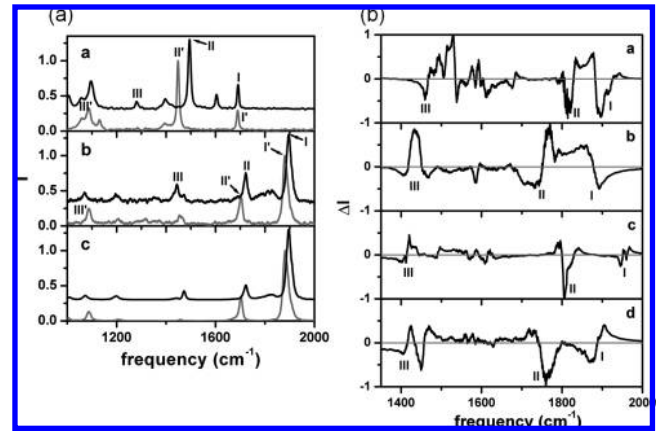

FIGURE 4. (a) Normalized IR spectra of NMA (black) and NMAD (gray) in aqueous solutions obtained from (trace a) classical MD simulations, (trace b) AM1/MM MD simulations with Mulliken charges for the solute, and (trace c) the time correlation function of C=O bond length from the AM1/MM MD trajectories. The amide modes of NMA are abbreviated as I, II, and III, respectively, while those of NMAD are primed. (b) VCD spectra of alanine dipeptide analogue in water calculated using QM/MM MD trajectory represented by (trace a) P_{II}, (trace b) RHH, (trace c) PB, and (trace d) coil conformations.

reproduce the amide band positions quite close to the experimental results, but the relative intensities and the inhomogeneous band broadening show larger deviation. On the contrary, the IR spectral profile in Figure 4(a)-b obtained from the AM1/MM MD simulations agrees well with experimental results. The relative intensities are in the order amide I−II−III, and the amide I bandwidth of 26 cm^{-1} is close to the experimental value of 29 cm^{-1}.[15] The band frequencies, however, should be properly scaled to the experimental values. The discrepancy in the band frequencies is expected to decrease if the QM level and the population analysis method are improved. The amide modes were assigned by comparing the IR spectrum with Fourier-transformed spectra of the autocorrelation functions of the relevant bond lengths and bending angles. In Figure 4(a)-c, the autocorrelation function of the C=O bond length of NMA obtained from the AM1/MM MD simulations is Fourier-transformed to produce the corresponding power spectrum. It clearly shows that the amide I mode of NMA in water is mainly due to C=O stretching and the amide II and III modes are due to C−N stretching and N−H in-plane bending.

The alanine dipeptide analogue (Ac-Ala-NHMe) is a prototype model of optically active peptides for the study of structure−spectrum relationship. The VCD spectra of the dipeptide in water were simulated by Fourier-transforming the cross-correlation function of the solute electric and magnetic dipole moments.[16] The restricted Hartree−Fock level with the basis sets 3-21G, 6-31G, and 6-31G* for a QM solute and

Downloaded by RENMIN UNIV OF CHINA on October 2, 2009 | http://pubs.acs.org
Publication Date (Web): May 20, 2009 | doi: 10.1021/ar900014e

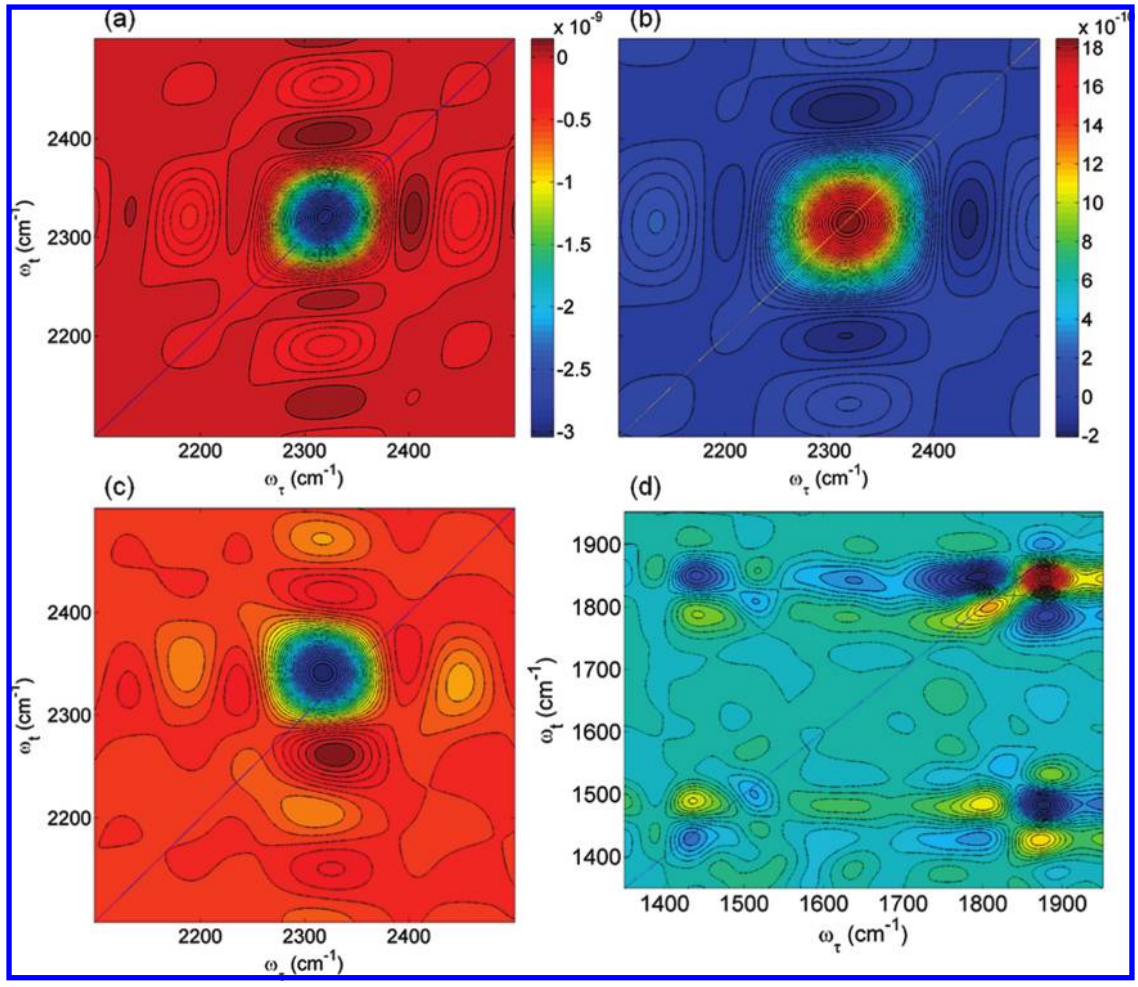

FIGURE 5. 2D IR absorptive spectra of CO and deuterated NMA in water clusters from QM/MM MD simulation and the classical third order response function. (a) Contribution from the first term of the CO response function. (b) Contribution from the second term. (c) CO spectrum as the sum of (a) and (b). (d) NMA spectrum from the entire response function.

Downloaded by RENMIN UNIV OF CHINA on October 2, 2009 | http://pubs.acs.org
Publication Date (Web): May 20, 2009 | doi: 10.1021/ar900014e

TIP3P for water was used. The fluctuating atomic partial charges were obtained from the Löwdin population analysis. Each MD trajectory is started at either RHH or fully extended conformation. Trajectories dominantly populated with a secondary conformation such as P_{II}, RHH, parallel or antiparallel β-strand, or C_7^{eq} are chosen to simulate the corresponding VCD spectra in Figure 4(b). The simulated VCD spectrum with a P_{II}-dominant trajectory in Figure 4(b)-a is compatible with previous experimental results of polyproline peptides,[53] where the amide I and II VCD bands are negative couplets with a weak positive peak to the high frequency region. The simulated VCD spectrum of RHH in Figure 4(b)-b has the reverse sign pattern compared to the P_{II} spectrum and successfully reproduces most of the salient features of experimental VCD spectra of RHH polypeptides and proteins. The reverse sign pattern of the amide I VCD spectra of P_{II} and RHH is reproduced even with relatively short trajectories. The line shape and sign patterns of the β-strand VCD spectrum in Figure 4(b)-c are qualitatively similar to the experimental spectra of β-sheet rich proteins. Interestingly, we found that the simulated VCD spectra of P_{II}, PB, and coil conformations have qualitatively similar sign patterns and spectral profiles. The amide II VCD bands, however, are commonly overestimated in those spectra and are stronger than the amide I VCD. The present study, as the first one adopting the QM/MM MD method to simulate VCD spectra, demonstrates that the negative couplet structures of the amide I and II VCD spectra do not necessarily prove the dominance of either P_{II} or coil conformation.

2D IR Spectroscopy with Classical Approximation and QM/MM MD Method

Classical Approximation of Electric Dipole Nonlinear Response Function. The third order response function relevant to the 2D IR spectroscopy ($n = 3$ in eq 1) can be expressed, within the electric dipole approximation, as the ensemble-averaged nested quantum commutators involving

dipole operators at different times.[11] In the classical limit, the quantum commutators are replaced by Poisson brackets

$$[A, B] \rightarrow i\hbar\{A, B\}_{PB} \quad (14)$$

and the response function becomes

$$R^{(3)}_{\alpha\beta\gamma\delta}(t_3, t_2, t_1) = \beta \mathrm{Tr}[\{\mu_\alpha(t_1 + t_2 + t_3), \mu_\beta(t_1 + t_2)\}_{PB}(\{\mu_\gamma(t_1), \dot{\mu}_\delta(0)\}_{PB} - \beta\dot{\mu}_\gamma(t_1)\,\dot{\mu}_\delta(0))\rho_{eq}] \quad (15)$$

in the canonical ensemble with density operator ρ_{eq}. Here, the Greek subscripts denote Cartesian components, μ represents the system dipole moment and $\dot{\mu}$ is its time derivative. Utilizing the invariance of Poisson brackets under canonical transformation and assuming that the dipole moment is a function of particle positions only, eq 15 can be evaluated numerically via the stability matrix of the trajectory.[17,54,55] The stability matrix computation is the critical and most time-consuming step in this classical formalism. For computational efficiency, the reverse trajectory obtained by changing the signs of momenta at time t_0 was used for the time evolution in t_1, while t_2- and t_3-evolutions were followed using the forward trajectory.[55]

The classical third order response function has been investigated using simple periodic model systems[56,57] and it is known to diverge in at least one particular direction in the two-dimensional space spanned by t_1 and t_3. However, once the chromophore is placed in liquid, the corresponding classical response function is generally believed to converge.[58]

2D IR Spectroscopy of CO and NMA in Water. $R^{(3)}$ in eq 15 can be shown to vanish for a harmonic oscillator as is well-known for its quantum counterpart. This indicates that conventional classical force fields based on harmonic intramolecular potential might fail to produce 2D IR signal. MD simulation of an NMA in liquid water with the OPLS-AA force field confirmed this.[55] Although each of the two terms in eq 15 produces distinctive peaks in the calculated 2D IR spectra, they cancel each other and the total signal becomes vanishingly small. Furthermore, We note that the harmonic nature of classical intramolecular potential functions is hardly changed by the anharmonic intermolecular interactions. To accurately calculate the response function, it is thus essential to employ high quality force fields that are capable of properly describing such potential anharmonicities. For this purpose, QM/MM force fields with semiempirical QM models could be adequate, considering the accuracy of model and the computational cost.

SCHEME 1. Schematic Chart for Computational Vibrational Spectroscopy[a]

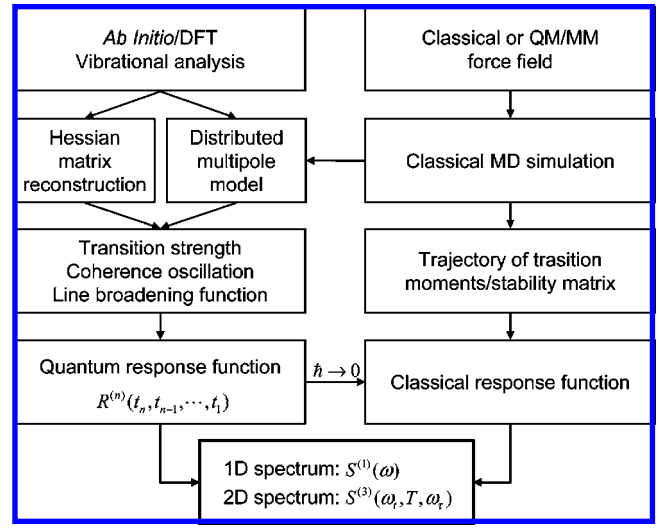

[a] The procedure of the hybrid ESC/MD (left) and the direct classical MD (right) methods are shown.

Figure 5 presents the 2D IR spectra of CO and deuterated NMA inside a water cluster containing 400 water molecules. PM3 model for the NMA and a classical flexible water model were employed. In Figure 5(a),(b), the two contributions of $R^{(3)}$ in eq 15 are plotted and they produce strong peaks of opposing sign near the CO stretching frequency of 2320 cm^{-1}. Note that the two peaks from the first and second terms of $R^{(3)}$ in eq 15 are displaced by ~4 cm^{-1} from each other, as shown in Figure 5(a),(b), and this causes the doublet splitting in the total spectrum in Figure 5(c). Although the doublet peaks do not align along the vertical axis, it clearly resembles the typical vertical splitting patterns found in many experimental 2D IR spectra of a-single-anharmonic-oscillator systems. Figure 5(d) shows the 2D IR spectrum of deuterated NMA in heavy water. The strong peak near 1900 cm^{-1} corresponds to the amide I mode. In general, the classical response functions converge very slowly and it would require very long sampling and further analysis to draw firm conclusions from the spectra. Nevertheless, the strong presence of the diagonal amide I peak and its cross peak with the 1430 cm^{-1} band suggest that this method could be quite useful when analyzing multimode 2D IR spectrum.

Concluding Remarks

The computational methods presented in this Account can be summarized by Scheme 1. The hybrid ESC/MD method provides a reliable way to calculate 1D and 2D vibrational spectra of specific modes with accurate fundamental vibrational properties and realistic solvent effects. The direct MD

Downloaded by RENMIN UNIV OF CHINA on October 2, 2009 | http://pubs.acs.org
Publication Date (Web): May 20, 2009 | doi: 10.1021/ar900014e

method evaluates the classical analogue of the vibrational response function and, despite being more demanding computationally, provides vibrational spectra reflecting the entire range of dynamical events. Since the two methods are quite different in their strengths, they can be utilized in a complementary way to understand vibrational spectroscopy and uncover its potentials. In the present Account, a few applications to amide modes of peptides and proteins have been described.

Computational vibrational spectroscopy will continue to advance in its methodology and to be applied to study a wide range of chemical and biological processes. Specifically, the hybrid method is suitably positioned to study vibrations of various marker modes of peptides and proteins. This will be of critical use in interpreting multidimensional vibrational spectra of complex molecules and provide even richer information on protein dynamics. The direct method, with further characterization of its classical approximation and methodological development, can be fruitfully used to study vibrational spectra of large molecules including proteins and their intermode interactions.

This work was supported by Creative Research Initiatives (CMDS) of MEST/KOSEF.

BIOGRAPHICAL INFORMATION

Jonggu Jeon received a Ph.D. in 2001 from Carnegie Mellon University under Hyung J. Kim. After postdoctoral research in the U.S.A. and Korea, he has been a research professor at Korea University since 2007.

Seongeun Yang received her Ph.D. in 2000 at Seoul National University in Seoul, Korea. She has been working as a research professor at Korea University since 2003.

Jun-Ho Choi received a Ph.D. in 1996 from Seoul National University in Korea under the direction of Sangyoub Lee. He has been working as a research professor at Korea University since 2000.

Minhaeng Cho received a Ph.D. from University of Chicago in 1993 under the direction of Prof. Graham R. Fleming. After 2 years of postdoctoral training at MIT in Prof. Robert J. Silbey's group, he has been on the faculty of Korea University since 1996.

FOOTNOTES

*To whom correspondence should be addressed. E-mail: mcho@korea.ac.kr.

REFERENCES

1 Ernst, R. R.; Bodenhausen, G.; Wokaun, A. *Nuclear Magnetic Resonance in One and Two Dimensions*; Oxford University Press: Oxford, 1987.

2 Hamm, P.; Lim, M.; Hochstrasser, R. M. Structure of the amide I band of peptides measured by femtosecond nonlinear-infrared spectroscopy. *J. Phys. Chem. B* **1998**, *102*, 6123–6138.

3 Tanimura, Y.; Mukamel, S. Two-Dimensional Femtosecond Vibrational Spectroscopy of Liquids. *J. Chem. Phys.* **1993**, *99*, 9496–9511.

4 Park, K.; Cho, M. Time- and frequency-resolved coherent two-dimensional IR spectroscopy: Its complementary relationship with the coherent two-dimensional Raman scattering spectroscopy. *J. Chem. Phys.* **1998**, *109*, 10559–10569.

5 Cho, M. Two-Dimensional Vibrational Spectroscopy. In *Advances in Multi-Photon Processes and Spectroscopy*; Lin, S. H., Villaeys, A. A., Fujimura, Y., Eds.; World Scientific Pulblishing Co.: Singapore, 1999; Vol. 12; pp 229−300.

6 Mukamel, S. Multidimensional femtosecond correlation spectroscopies of electronic and vibrational excitations. *Annu. Rev. Phys. Chem.* **2000**, *51*, 691–729.

7 Cho, M. Ultrafast vibrational spectroscopy in condensed phases. *PhysChemComm* **2002**, 40–58.

8 Cho, M. Coherent two-dimensional optical spectroscopy. *Chem. Rev.* **2008**, *108*, 1331–1418.

9 Zheng, J.; Kwak, K.; Fayer, M. D. Ultrafast 2D IR Vibrational Echo Spectroscopy. *Acc. Chem. Res.* **2007**, *40*, 75–83.

10 Ganim, Z.; Chung, H. S.; Smith, A. W.; DeFlores, L. P.; Jones, K. C.; Tokmakoff, A. Amide I Two-Dimensional Infrared Spectroscopy of Proteins. *Acc. Chem. Res.* **2008**, *41*, 432–441.

11 Mukamel, S. *Principles of Nonlinear Optical Spectroscopy*; Oxford University Press: Oxford, 1995.

12 Ham, S.; Kim, J. H.; Lee, H.; Cho, M. Correlation between electronic and molecular structure distortions and vibrational properties. II. Amide I modes of NMA-nD_2O complexes. *J. Chem. Phys.* **2003**, *118*, 3491–3498.

13 Choi, J.-H.; Lee, H.; Lee, K.-K.; Hahn, S.; Cho, M. Computational spectroscopy of ubiquitin: Comparison between theory and experiments. *J. Chem. Phys.* **2007**, *126*, 045102.

14 McQuarrie, D. A. *Statistical Mechanics*; Harper & Row: New York, 1976.

15 Yang, S.; Cho, M. IR spectra of N-methylacetamide in water predicted by combined quantum mechanical/molecular mechanical molecular dynamics simulations. *J. Chem. Phys.* **2005**, *123*, 134503.

16 Yang, S.; Cho, M. Simulations of Infrared and Vibrational Circular Dichroism Spectra Using Dynamic Partial Charges Obtained from QM/MM Molecular Dynamics: Alanine Dipeptide Analogue in Water. Submitted for publication.

17 Mukamel, S.; Khidekel, V.; Chernyak, V. Classical chaos and fluctuation-dissipation relations for nonlinear response. *Phys. Rev. E* **1996**, *53*, R1−R4.

18 Ma, A.; Stratt, R. M. Fifth-Order Raman Spectrum of an Atomic Liquid: Simulation and Instantaneous-Normal-Mode Calculation. *Phys. Rev. Lett.* **2000**, *85*, 1004–1007.

19 Hasegawa, T.; Tanimura, Y. Calculating fifth-order Raman signals for various molecular liquids by equilibrium and nonequilibrium hybrid molecular dynamics simulation algorithms. *J. Chem. Phys.* **2006**, *125*, 074512.

20 Nagata, Y.; Tanimura, Y.; Mukamel, S. Two-dimensional infrared surface spectroscopy for CO on Cu(100): Detection of intermolecular coupling of adsorbates. *J. Chem. Phys.* **2007**, *126*, 204703.

21 Okumura, K.; Tanimura, Y. Femtosecond two-dimensional spectroscopy from anharmonic vibrational modes of molecules in the condensed phase. *J. Chem. Phys.* **1997**, *107*, 2267–2283.

22 *Combined Quantum Mechanical and Molecular Mechanical Methods*; Gao, J., Thompson, M. A., Eds.; ACS Symposium Series 712; American Chemical Society: Washington, DC, 1998.

23 Kim, Y. S.; Liu, L.; Axelsen, P. H.; Hochstrasser, R. M. Two-dimensional infrared spectra of isotopically diluted amyloid fibrils from Aβ40. *Proc. Natl. Acad. Sci. U.S.A.* **2008**, *105*, 7720–7725.

24 Schweitzer-Stenner, R. Advances in vibrational spectroscopy as a sensitive probe of peptide and protein structure: A critical review. *Vib. Spectrosc.* **2006**, *42*, 98–117.

25 Mukherjee, P.; Kass, I.; Arkin, I. T.; Zanni, M. T. Picosecond dynamics of a membrane protein revealed by 2D IR. *Proc. Natl. Acad. Sci. U.S.A.* **2006**, *103*, 3528–3533.

26 Ham, S.; Cha, S.; Choi, J.-H.; Cho, M. Amide I modes of tripeptides: Hessian matrix reconstruction and isotope effects. *J. Chem. Phys.* **2003**, *119*, 1451–1461.

27 Choi, J.-H.; Kim, J.-S.; Cho, M. Amide I vibrational circular dichroism of polypeptides: Generalized fragmentation approximation method. *J. Chem. Phys.* **2005**, *122*, 174903.

28 Liptay, W. Dipole moments and polarizabilities of molecules in excited states. In *Excited States*; Lim, E. C., Ed.; Academic Press: New York, 1974; Vol. 1; pp 129−229.

29 Bublitz, G. U.; Boxer, S. G. STARK SPECTROSCOPY: Applications in Chemistry, Biology, and Materials Science. *Annu. Rev. Phys. Chem.* **1997**, *48*, 213–242.

30 Cho, M. Vibrational solvatochromism and electrochromism: Coarse-grained models and their relationships. *J. Chem. Phys.* **2009**, *130*, 094505.

31 Ham, S.; Cho, M. Amide I modes in the N-methylacetamide dimer and glycine dipeptide analog: Diagonal force constants. *J. Chem. Phys.* **2003**, *118*, 6915–6922.

Downloaded by RENMIN UNIV OF CHINA on October 2, 2009 | http://pubs.acs.org
Publication Date (Web): May 20, 2009 | doi: 10.1021/ar900014e

32 Schmidt, J. R.; Corcelli, S. A.; Skinner, J. L. Ultrafast vibrational spectroscopy of water and aqueous N-methylacetamide: Comparison of different electronic structure/molecular dynamics approaches. *J. Chem. Phys.* **2004**, *121*, 8887–8896.

33 Jansen, T. l. C.; Knoester, J. A transferable electrostatic map for solvation effects on amide I vibrations and its application to linear and two-dimensional spectroscopy. *J. Chem. Phys.* **2006**, *124*, 044502.

34 Zhuang, W.; Abramavicius, D.; Hayashi, T.; Mukamel, S. Simulation Protocols for Coherent Femtosecond Vibrational Spectra of Peptides. *J. Phys. Chem. B* **2006**, *110*, 3362–3374.

35 Hush, N. S.; Reimers, J. R. Vibrational Stark Spectroscopy. 1. Basic Theory and Application to the CO Stretch. *J. Phys. Chem.* **1995**, *99*, 15798–15805.

36 Suydam, I. T.; Boxer, S. G. Vibrational Stark Effects Calibrate the Sensitivity of Vibrational Probes for Electric Fields in Proteins. *Biochemistry* **2003**, *42*, 12050–12055.

37 Andrews, S. S.; Boxer, S. G. Vibrational Stark Effects of Nitriles I. Methods and Experimental Results. *J. Phys. Chem. A* **2000**, *104*, 11853–11863.

38 Suydam, I. T.; Snow, C. D.; Pande, V. S.; Boxer, S. G. Electric Fields at the Active Site of an Enzyme: Direct Comparison of Experiment with Theory. *Science* **2006**, *313*, 200–204.

39 Choi, J.-H.; Oh, K.-I.; Lee, H.; Lee, C.; Cho, M. Nitrile and thiocyanate IR probes: Quantum chemistry calculation studies and multivariate least-square fitting analysis. *J. Chem. Phys.* **2008**, *128*, 134506.

40 Choi, J.-H.; Oh, K.-I.; Cho, M. Azido-derivatized compounds as IR probes of local electrostatic environment: Theoretical studies. *J. Chem. Phys.* **2008**, *129*, 174512.

41 This experimental value was obtained with azidotrimethylsilane, not methylazide.

42 Choi, J.-H.; Hahn, S.; Cho, M. Vibrational spectroscopic characteristics of secondary structure polypeptides in liquid water: Constrained MD simulation studies. *Biopolymers* **2006**, *83*, 519–536.

43 Jansen, T. l. C.; Knoester, J. Nonadiabatic Effects in the Two-Dimensional Infrared Spectra of Peptides: Application to Alanine Dipeptide. *J. Phys. Chem. B* **2006**, *110*, 22910–22916.

44 Gorbunov, R. D.; Nguyen, P. H.; Kobus, M.; Stock, G. Quantum-classical description of the amide I vibrational spectrum of trialanine. *J. Chem. Phys.* **2007**, *126*, 054509.

45 Choi, J.-H.; Cheon, S.; Lee, H.; Cho, M. Two-dimensional nonlinear optical activity spectroscopy of coupled multi-chromophore system. *Phys. Chem. Chem. Phys.* **2008**, *10*, 3839–3856.

46 Huang, R.; Kubelka, J.; Barber-Armstrong, W.; Silva, R. A. G. D.; Decatur, S. M.; Keiderling, T. A. Nature of vibrational coupling in helical peptides: An isotopic labeling study. *J. Am. Chem. Soc.* **2004**, *126*, 2346–2354.

47 Woutersen, S.; Hamm, P. Time-resolved two-dimensional vibrational spectroscopy of a short α helix in water. *J. Chem. Phys.* **2001**, *115*, 7737–7743.

48 Zanni, M. T.; Ge, N.-H.; Kim, Y. S.; Hochstrasser, R. M. Two-dimensional IR spectroscopy can be designed to eliminate the diagonal peaks and expose only the crosspeaks needed for structure determination. *Proc. Natl. Acad. Sci. U.S.A.* **2001**, *98*, 11265–11270.

49 Hahn, S.; Kim, S.-S.; Lee, C.; Cho, M. Characteristic two-dimensional IR spectroscopic features of antiparallel and parallel beta-sheet polypeptides: Simulation studies. *J. Chem. Phys.* **2005**, *123*, 084905.

50 Abramavicius, D.; Mukamel, S. Chirality-induced signals in coherent multidimensional spectroscopy of excitons. *J. Chem. Phys.* **2006**, *124*, 034113.

51 Gao, J. Methods and applications of combined quantum mechanical and molecular mechanical potentials. In *Rev. Comput. Chem.*; Lipkowitz, K. B., Boyd, D. B., Eds.; VCH Publishers, Inc.: New York, 1996; Vol. 7; pp 119—185.

52 Rhee, H.; Ha, J.-H.; Jeon, S.-J.; Cho, M. Femtosecond spectral interferometry of optical activity: Theory. *J. Chem. Phys.* **2008**, *129*, 094507.

53 Bour, P.; Keiderling, T. A. Ab initio simulations of the vibrational circular dichroism of coupled peptides. *J. Am. Chem. Soc.* **1993**, *115*, 9602–9607.

54 Williams, R. B.; Loring, R. F. Classical mechanical photon echo of a solvated anharmonic vibration. *J. Chem. Phys.* **2000**, *113*, 1932–1941.

55 Jeon, J.; Cho, M. In preparation.

56 Noid, W. G.; Ezra, G. S.; Loring, R. F. Vibrational Echoes: Dephasing, Rephasing, and the Stability of Classical Trajectories. *J. Phys. Chem. B* **2004**, *108*, 6536–6543.

57 Kryvohuz, M.; Cao, J. Classical Divergence of Nonlinear Response Functions. *Phys. Rev. Lett.* **2006**, *96*, 030403.

58 Dellago, C.; Mukamel, S. Simulation algorithms for multidimensional nonlinear response of classical many-body systems. *J. Chem. Phys.* **2003**, *119*, 9344–9354.

Downloaded by RENMIN UNIV OF CHINA on October 2, 2009 | http://pubs.acs.org
Publication Date (Web): May 20, 2009 | doi: 10.1021/ar900014e